Modeling of Offshore Crane and Marine Craft in Wave Motion

Ronny Landsverk[1], Jing Zhou[2] and Geir Hovland[3]
Faculty of Engineering and Science
University of Agder
Grimstad, Norway 4879
emails: [1] *ronny.landsverk@uia.no;*
[2]*jing.zhou@uia.no;*
[3]*geir.hovland@uia.no*

Houxiang Zhang
Department of Ocean Operations
and Civil Engineering
Norwegian University of Science and Technology
Ålesund, Norway
email: hozh@ntnu.no

***Abstract*—Safe handling of heavy payloads in an offshore environment requires careful planning and depends on the interaction between a crane and a vessel. This paper investigates the coupled dynamics between a multipurpose crane with payload, and an offshore carrying vessel. A classical multibody model is derived using holonomic constraints and Newton-Euler kinetics. The resulting index-3 system of differential-algebraic equation (DAE) is transformed into an index-1 system and solved using commonly used numerical ode solvers. Numerical simulations are carried out to show that the proposed models behave in a physically realistic manner.**

***Keywords*-mathematical modeling, offshore cranes, multibody dynamics, Newton-Euler method, marine craft**

I. Introduction

Vessel-mounted cranes are important for several offshore industries, e.g. offshore drilling and windmill farms. The conventional knuckle-boom crane is multipurpose, and has remarkable lifting capabilities, but requires experienced personnel and a lot of planning when significantly heavy payloads are involved. In a worst case scenario, a heavy lifting operation can impact the vessel stability and dangerous situations and high-cost failures may follow. On the contrary, marine craft designers and regulatory decision makers may be conservative regarding allowable crane loads and weather windows, which in turn lead to higher costs associated with the size of the vessel and downtime due to bad weather. Hence, there is a need to further investigate the coupled dynamics between the crane and vessel, and to seek more autonomy in a control setting.

Over the past decade, modeling and control of cranes have been extensively studied. In [1], a Lagrangian-based dynamic model of a ship-mounted boom crane was derived about a vessel-fixed reference frame, and appended inertial forces and moments using relative accelerations of various points. This paper was further developed with focus on offshore crane control in [2] and [3]. In above papers, the ship was assumed to move only in roll and heave, and furthermore to be sufficiently large to not be affected by the crane-payload system

In [4], a moored crane-vessel with suspended load was analyzed both analytically and experimentally. In this study, a 4 degrees of freedom rigid-body model of the ship was influenced by mooring forces, viscous drag and frequency-dependent wave forces. The hydrodynamics was included by introducing additional state space models based on pre-simulations using the software WAMIT. The resulting time-domain model and a corresponding frequency domain model were used to study nonlinear dynamic phenomena affected by the mooring stiffness in particular. This study was relevant for investigating how wave excitation affect surge and payload swing motion. The problem is that the crane itself remains static and that the degree of freedom most sensitive to disturbances, i.e. the roll, is not considered.

In [5] and [6], a fully coupled spatial knuckle-boom crane on a marine craft was modelled using Kane's method, using a minimal set of coordinates and generalized speeds. In above works, partial velocities needed for Kane's equations were defined as screws which enable screw transformations as a means to project kinetics to the inertial frame. Constraint forces/moments were cancelled from the equations of motion using D'Alembert's principle and virtual work, and in [6], brought back into evidence using screw transformations. In this work, the crane was modelled as a serial link manipulator, thereby avoiding the closed loops that arise by including cylinder kinetics.

In this paper, we propose to use a classical multibody dynamics formulation with a full set of Cartesian coordinates and Euler angles for each body to derive a fully coupled model of vessel, crane and payload. Equations of motion are derived using a Newton-Euler formulation and appended with holonomic kinematic constraints to reach the desired number of degrees of freedom. Wave loads and hydrodynamic parameters for the vessel are obtained from pre-simulations using the hydrodynamic code VERES [7], implementing 2D strip

theory as described in [8]. Kinematic singularities associated with Euler-angles are accounted for by specifying suitable initial orientations of the body-frames. The multi-body system consists of ten rigid bodies, including the vessel and payload. Hence, the crane is built up by eight moving bodies, where the base of the crane is rigidly fixed to the deck of the vessel. Using the methods proposed, we overcome the difficulties in including the closed kinematic loops associated with the two cylinders of the crane, and with the king, main jib and knuckle-jib, the system makes up a typical multipurpose offshore knuckle-boom crane. Constraint forces and moments are expressed using Lagrange multipliers and included in the formulation, which is numerically efficient and convenient for in-depth analysis of forces acting between individual members. The final model description yields an index-1 DAE system which is simulated using MATLAB's ode solver package.

II. Modeling of Crane and Marine Craft

A. Crane Model

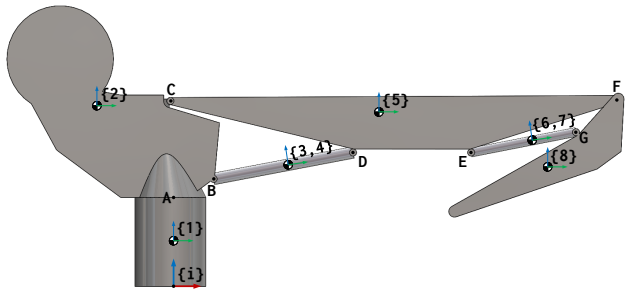

Figure 1: Lumped Rigid Bodies and Points of Interest

Large conventional knuckle-boom cranes are highly complex and consist of many moving parts. For our case study, we care mostly about the gross rigid-body dynamics, and hence are willing to make a lot of simplifications. In particular, the winch, sheaves, etc are considered to be statically fixed to relevant bodies. The simplified crane consists of eight bodies, as shown in figure 1. There are two heavy-duty hydraulic cylinders, which eventually require inclusion of pressure-volumes and valve control, but for this case, we consider their kinetics only and neglect the means of power supply. Likewise for the base revolute joint A, we assume that torque is supplied in an ideal manner.

The pose of each body is described by six coordinates, where three are along cartesian axes (x, y, z), and three are the rotations about these axes, (ϕ_x, ϕ_y, ϕ_z).Any set of such rotations will be associated with a singularity. Using XYZ order of rotation, this singularity will occur if $\phi_y = (2n+1)\pi/2$, so we have placed all local y-axes accordingly (see figures 1 and 2). The crane (not considering payload or marine craft) should have three degrees of freedom. For a cartesian formulation, each body requires six coordinates for the pose to be fully defined. The system must satisfy

$$n_{\text{coord}} - n_{\text{con}} = n_{\text{dof}}$$

where $n_{\text{coord}}, n_{\text{con}}, n_{\text{dof}}$ are the number of coordinates, constraints and degrees of freedom, respectively - or equivalently, we must find $8 \cdot 6 - 3 = 45$ independent constraint equations. These are systematically found by defining joints as follows:

- Revolute joints at A, C and F
- Prismatic joints between bodies $3, 4$ and $6, 7$
- Infinitely strong weld between the deck and body-1
- Spherical joints at D and G
- Universal joints at B and E

Methods of describing such joints are given in [9], [10]. In total, going from the first to last item, these constraints form $3{\cdot}5{+}2{\cdot}5{+}1{\cdot}6{+}2{\cdot}3{+}2{\cdot}4 = 45$ equations, which is our target number for the crane. The payload is attached to the crane-tip using a so-called *spherical-spherical* joint, which can be regarded as a constant-distance constraint. It requires only one scalar equation, and therefore, the payload will have five degrees of freedom. Another way to interpret this is that we have a rigid link with no mass connected to a spherical joint at the payload via a spherical joint at the crane-tip.

B. Mathematical Model

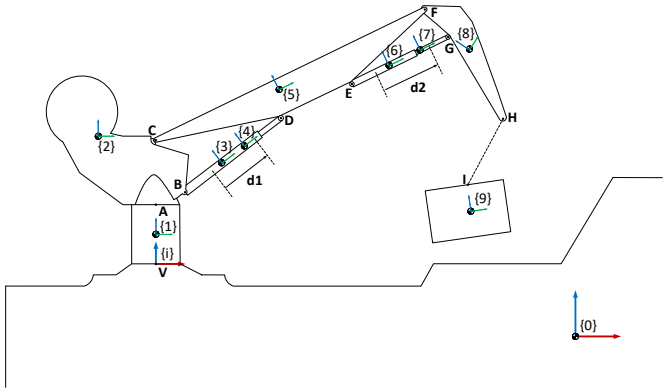

Figure 2: Appended model

The system kinematics is described by holonomic constraints of the form

$$\mathbf{\Phi}(\mathbf{q}) = \mathbf{0} \tag{1}$$

where $\mathbf{\Phi} \in \mathbb{R}^{n_{\text{con}}}$ is a vector function of the coordinate vector $\mathbf{q} \in \mathbb{R}^{n_{\text{coord}}}$. Using Cartesian coordinates, $\mathbf{r}^T = (x, y, z)$ and Euler angles, $\boldsymbol{\varphi}^T = (\phi_x, \phi_y, \phi_z)$, we

have $n_{\text{con}} = 46$ and $n_{\text{coord}} = 60$ for the fully coupled system (45 constraints for the crane-vessel and 1 for the payload). By differentiating eq. (1) wrt time t, assuming $\mathbf{\Phi}$ does not depend explicitly on t, we get

$$\frac{d\mathbf{\Phi}}{dt} = \frac{\partial \mathbf{\Phi}}{\partial \mathbf{q}} \frac{d\mathbf{q}}{dt} + \frac{\partial \mathbf{\Phi}}{\partial t} = \mathbf{\Phi_q}\dot{\mathbf{q}} = \mathbf{0} \tag{2}$$

which can be rewritten as

$$\mathbf{\Phi_q}\dot{\mathbf{q}} = \mathbf{D}(\mathbf{q}) \begin{bmatrix} \dot{\mathbf{r}}_0 \\ \boldsymbol{\omega}_0 \\ \vdots \\ \dot{\mathbf{r}}_9 \\ \boldsymbol{\omega}_9 \end{bmatrix} = \mathbf{0} \tag{3}$$

where $\mathbf{D}(\mathbf{q})$ is a manipulated Jacobian matrix and $\mathbf{r}_i$ and $\boldsymbol{\omega}_i$, $i = 0, ..., 9$ are the global position vectors and angular velocities of each body i. The step going from $\mathbf{\Phi_q}\dot{\mathbf{q}}$ to $\mathbf{D}\left[\dot{\mathbf{r}}_0^T \cdots \boldsymbol{\omega}_9^T\right]^T$ in eq. (3) is based on the fact that spatial angular velocities are different from the rates of change of Euler angles. Rather, we must implement a transformation, i.e. $\dot{\boldsymbol{\varphi}} = \mathbf{T}(\boldsymbol{\varphi})\boldsymbol{\omega}$. A representative single-body version is illuminated by

$$\mathbf{\Phi_q} \begin{bmatrix} \dot{\mathbf{r}} \\ \dot{\boldsymbol{\varphi}} \end{bmatrix} = \mathbf{\Phi_q} \begin{bmatrix} \mathbf{I} & \mathbf{0} \\ \mathbf{0} & \mathbf{T} \end{bmatrix} \begin{bmatrix} \dot{\mathbf{r}} \\ \boldsymbol{\omega} \end{bmatrix} = \mathbf{D} \begin{bmatrix} \dot{\mathbf{r}} \\ \boldsymbol{\omega} \end{bmatrix} \tag{4}$$

where $\mathbf{I}$ is the identity matrix and $\mathbf{T}(\boldsymbol{\varphi})$ depends on the chosen order of Euler-angle rotations. The form used in this paper is derived in eq. (20).

The dynamics of the system is described using the Newton-Euler formulation. The general model for one constrained rigid body for center-of-mass acceleration is

$$\begin{bmatrix} m\mathbf{I} & \mathbf{0} \\ \mathbf{0} & \mathbf{J} \end{bmatrix} \begin{bmatrix} \ddot{\mathbf{r}} \\ \dot{\boldsymbol{\omega}} \end{bmatrix} + \begin{bmatrix} \mathbf{0} \\ \tilde{\boldsymbol{\omega}}\mathbf{J}\boldsymbol{\omega} \end{bmatrix} = \begin{bmatrix} \mathbf{f}^{\text{ext}} \\ \mathbf{n}^{\text{ext}} \end{bmatrix} + \begin{bmatrix} \mathbf{f}^c \\ \mathbf{n}^c \end{bmatrix} \tag{5}$$

where m is the mass, $\mathbf{r}$ is the position vector of the body-frame, $\mathbf{J}$ is the inertia matrix relative to the same frame for which we express the angular velocity $\boldsymbol{\omega}$. The tilde-operator denotes the skew-symmetric form of the vector-argument. Hence a matrix equation, $\tilde{\mathbf{a}}\mathbf{b}$, yields an algebraic form of the cross product, $\vec{a} \times \vec{b}$. Finally, the right-hand side forces/moments, $\mathbf{f}/\mathbf{n}$, are split into an external part and a part that represents the reaction forces between the bodies.

Using the theorem of Lagrange multipliers from linear algebra, we can express the constraint forces as a linear combination of the rows of the constraint Jacobian matrix, $\mathbf{D}$, or equivalently, as the linear combination of the columns of it's transpose:

$$\begin{bmatrix} \mathbf{f}^c \\ \mathbf{n}^c \end{bmatrix} = \mathbf{D}^T \boldsymbol{\lambda} \tag{6}$$

where $\boldsymbol{\lambda}$ is a column vector of Lagrange multipliers. Furthermore, since the kinematic constraints are linear in velocity and acceleration, we can derive an equation

$$\mathbf{D} \begin{bmatrix} \ddot{\mathbf{r}} \\ \dot{\boldsymbol{\omega}} \end{bmatrix} + \dot{\mathbf{D}} \begin{bmatrix} \dot{\mathbf{r}} \\ \boldsymbol{\omega} \end{bmatrix} = \mathbf{0} \quad \Rightarrow \quad \mathbf{D} \begin{bmatrix} \ddot{\mathbf{r}} \\ \dot{\boldsymbol{\omega}} \end{bmatrix} = \boldsymbol{\gamma} \tag{7}$$

where $\boldsymbol{\gamma}$ takes the form

$$\boldsymbol{\gamma} = -\dot{\mathbf{D}} \begin{bmatrix} \dot{\mathbf{r}} \\ \boldsymbol{\omega} \end{bmatrix} \tag{8}$$

Hence, we have a system of equations

$$\begin{bmatrix} \begin{bmatrix} m\mathbf{I} & \mathbf{0} \\ \mathbf{0} & \mathbf{J} \end{bmatrix} & -\mathbf{D}^T \\ \mathbf{D} & \mathbf{0} \end{bmatrix} \begin{bmatrix} \begin{bmatrix} \ddot{\mathbf{r}} \\ \dot{\boldsymbol{\omega}} \end{bmatrix} \\ \boldsymbol{\lambda} \end{bmatrix} = \begin{bmatrix} \begin{bmatrix} \mathbf{f}^{\text{ext}} \\ \mathbf{n}^{\text{ext}} - \tilde{\boldsymbol{\omega}}\mathbf{J}\boldsymbol{\omega} \end{bmatrix} \\ \boldsymbol{\gamma} \end{bmatrix} \tag{9}$$

For multi-body systems, the form of eq. (9) remains the same, and the majority of the workload lies in forming the kinematic equations that describe the interaction between the bodies, and differentiating these to get the constraint Jacobian and forming eq. (7). Note that this form is valid for mass center accelerations, with the angular velocity expressed relative to the inertial frame. This means that the inertia matrix $\mathbf{J}$ is expressed globally and is configuration-dependent, as in $\mathbf{J} = \mathbf{RIR}^T$, where the matrix $\mathbf{I}$ is the (constant) inertia matrix relative to the body-fixed frame, and $\mathbf{R} \in SO(3)$ is the rotation matrix relating the two frames.

C. Marine Craft Hydrodynamics

The marine craft model is based on parameters obtained from hydrodynamic pre-simulations using VERES/ShipX of a typical crane-carrying supply vessel. From the VERES theory manual, the linear coupled equations of motion for a marine craft can be written

$$\sum_{k=1}^{6} \left((M_{jk} + A_{jk})\, \ddot{\eta}_k + B_{jk}\dot{\eta}_k + C_{jk}\eta_k \right) = F_j \mathrm{e}^{i\omega t} \tag{10}$$

where $j = 1, ..., 6$ is the coordinate (surge, sway, heave, roll, pitch, yaw)

In eq. (10), the terms M_{jk} and A_{jk} represent mass and added mass, the term B_{jk} represent hydrodynamic damping and C_{jk} represents the restoring terms that involve the interaction between gravity and buoyancy. The right-hand side represents wave exciting forces/moments, for which the real part is physical. The frequency ω is the *encounter frequency*, but for a ship with zero velocity that frequency is the same as the wave frequency.

D. Kinematic Transformations

The vessel equations, as given in eq. (10), can be written in matrix form as

$$(\mathbf{M} + \mathbf{M}_A)\,\ddot{\boldsymbol{\eta}} + \mathbf{B}\dot{\boldsymbol{\eta}} + \mathbf{C}\boldsymbol{\eta} = \begin{bmatrix}\mathbf{f}^w \\ \mathbf{n}^w\end{bmatrix} \tag{11}$$

where $\mathbf{M}$ is the generalized mass matrix, $\mathbf{M}_A$ and $\mathbf{B}$ is the hydrodynamic added mass and damping, $\mathbf{C}$ is a hydrostatic restoring matrix, and the right-hand side consists of wave loads. The underlying theory that VERES uses assumes symmetry about the xz-plane, and a center-of-mass location $(0, 0, z_G)$ relative to the body-frame of the ship. It follows that the generalized mass matrix has the form

$$\mathbf{M} = \begin{bmatrix} m & 0 & 0 & 0 & mz_G & 0 \\ 0 & m & 0 & -mz_G & 0 & 0 \\ 0 & 0 & m & 0 & 0 & 0 \\ 0 & -mz_G & 0 & I_x & 0 & -I_{xz} \\ mz_G & 0 & 0 & 0 & I_y & 0 \\ 0 & 0 & 0 & -I_{xz} & 0 & I_z \end{bmatrix} \tag{12}$$

where m is the mass of the vessel. If the location of the body-frame is at $z_G = 0$, then the terms mz_G vanish. The added mass and damping matrices, $\mathbf{M}_A$, $\mathbf{B}$ are really frequency dependent, but this dependency will be dealt with in later sections, and the remaining parts are those that correspond to the highest wave frequency supplied to VERES. The hydrostatic matrix $\mathbf{C}$ has only five nonzero entries:

$$C_{33} = \rho g A_{wp} \tag{13}$$

$$C_{35} = C_{53} = -\rho g \int_L bx\,dx \tag{14}$$

$$C_{44} = \rho g \nabla \overline{GM}_T \tag{15}$$

$$C_{55} = \rho g \nabla \overline{GM}_L \tag{16}$$

where ρ is the fluid density, g is the gravitational constant, b is the breadth of the vessel, A_{wp} is the waterplane area, ∇ is the displaced water volume and $\overline{GM}_T$ and $\overline{GM}_L$ are the metacentric heights for the transversal and longitudal directions. If we write the coordinate vector $\boldsymbol{\eta}$ as $[\mathbf{r}^T, \boldsymbol{\varphi}^T]^T$ where $\boldsymbol{\varphi}$ are Euler-rotation angles, then, for consistency in our formulation, we should transform the leading term of eq (11) to have the form $\mathbf{M}\dot{\mathbf{v}}$ where $\mathbf{v}^T = [\dot{\mathbf{r}}^T, \boldsymbol{\omega}^T]$. We start by writing

$$\dot{\boldsymbol{\eta}} = \begin{bmatrix}\dot{\mathbf{r}} \\ \dot{\boldsymbol{\varphi}}\end{bmatrix} = \begin{bmatrix}\dot{\mathbf{r}} \\ \mathbf{T}(\boldsymbol{\varphi})\boldsymbol{\omega}\end{bmatrix} = \begin{bmatrix}\mathbf{I} & \mathbf{0} \\ \mathbf{0} & \mathbf{T}(\boldsymbol{\varphi})\end{bmatrix}\begin{bmatrix}\dot{\mathbf{r}} \\ \boldsymbol{\omega}\end{bmatrix} \tag{17}$$

where $\mathbf{T}(\boldsymbol{\varphi})$ is a transformation relating the rates of change of the Euler angles, $\dot{\boldsymbol{\varphi}}$, to the angular velocity vector $\boldsymbol{\omega}$. The matrix $\mathbf{T}(\boldsymbol{\varphi})$ is easily obtained by deriving it's inverse, by writing the angular velocity as a summation of simple rotations. Using an XYZ rotation sequence, where the individual rotations are about current body-axes, we can write

$$\boldsymbol{\omega} = {}^A\boldsymbol{\omega}^B + {}^B\boldsymbol{\omega}^C + {}^C\boldsymbol{\omega}^D \tag{18}$$

where the notation indicates rotation *from* the left superscript-frame and *to* the right superscript-frame, and the frames A and D are the inertial and body frames, and the frames B and C are intermediate frames. We then can write

$$\boldsymbol{\omega} = \dot{\phi}_x\hat{\mathbf{a}}_x + \dot{\phi}_y\hat{\mathbf{b}}_y + \dot{\phi}_z\hat{\mathbf{c}}_z \tag{19}$$

where we understand that the unit vectors belong to the matching frames. The result will give

$$\boldsymbol{\omega} = \begin{bmatrix}1 & 0 & 0 \\ 0 & \cos(\phi_x) & -\sin(\phi_x)\cos(\phi_y) \\ 0 & \sin(\phi_x) & \cos(\phi_x)\cos(\phi_y)\end{bmatrix}\begin{bmatrix}\dot{\phi}_x \\ \dot{\phi}_y \\ \dot{\phi}_z\end{bmatrix} = \mathbf{T}^{-1}\dot{\boldsymbol{\varphi}} \tag{20}$$

Then, the time derivative gives

$$\dot{\boldsymbol{\omega}} = \mathbf{T}^{-1}\ddot{\boldsymbol{\varphi}} + \frac{d\mathbf{T}^{-1}}{dt}\dot{\boldsymbol{\varphi}} \tag{21}$$

where

$$\frac{d\mathbf{T}^{-1}}{dt} = \dot{\mathbf{T}}^{-1} = \begin{bmatrix}0 & 0 & 0 \\ 0 & -s_x\dot{\phi}_x & -c_xc_y\dot{\phi}_x + s_xs_y\dot{\phi}_y \\ 0 & c_x\dot{\phi}_x & -s_xc_y\dot{\phi}_x - c_xs_y\dot{\phi}_y\end{bmatrix} \tag{22}$$

and furthermore, we can write

$$\ddot{\boldsymbol{\varphi}} = \mathbf{T}\dot{\boldsymbol{\omega}} - \mathbf{T}\dot{\mathbf{T}}^{-1}\dot{\boldsymbol{\varphi}} \tag{23}$$

and rewrite eq. (11) as

$$\mathbf{M}_0\begin{bmatrix}\ddot{\mathbf{r}} \\ \dot{\boldsymbol{\omega}}\end{bmatrix} + \mathbf{B}_0\begin{bmatrix}\dot{\mathbf{r}} \\ \boldsymbol{\omega}\end{bmatrix} + \mathbf{C}\boldsymbol{\eta} - \mathbf{b}_0 = \mathbf{F}\mathrm{e}^{i\omega t} \tag{24}$$

where

$$\mathbf{M}_0 = (\mathbf{M} + \mathbf{M}_A)\begin{bmatrix}\mathbf{I} & \mathbf{0} \\ \mathbf{0} & \mathbf{T}\end{bmatrix} \tag{25}$$

$$\mathbf{B}_0 = \mathbf{B}\begin{bmatrix}\mathbf{I} & \mathbf{0} \\ \mathbf{0} & \mathbf{T}\end{bmatrix} \tag{26}$$

$$\mathbf{b}_0 = (\mathbf{M} + \mathbf{M}_A)\begin{bmatrix}\mathbf{0} \\ \mathbf{T}\dot{\mathbf{T}}^{-1}\dot{\boldsymbol{\varphi}}\end{bmatrix} \tag{27}$$

E. Fluid Memory - Radiation Forces

The hydrodynamic loads acting on a structure in a seaway is classicly split into two parts; loads acting from wave excitations, or diffraction loads, and loads that result in fluid radiation as the moving structure displaces the surrounding water. Note that the equations (10) are only valid in steady state sinusoidal motions, and a more accurate simulation should include memory effects which incorporate transient dynamics. These fluid memory effects, μ, are related to the frequency dependence of

added mass and damping, and can be written as a convolution term

$$\mu_j = \sum_{k=1}^{6} \mu_{jk} = \sum_{k=1}^{6} \int_{-\infty}^{t} K_{jk}(t-\tau)\dot{\eta}_k(\tau)d\tau \tag{28}$$

where $j = 1, ..., 6$ and the convolution kernel, K_{jk} is regarded as the impulse response of $\dot{\eta}_k$. This convolution is impractical for numeric simulations, and Kristiansen, et.al [11] proposed to represent μ_{jk} as a state space model

$$\mu_{jk} = \mathbf{C}_{jk}\mathbf{x}_{jk} + D_{jk}\dot{\eta}_k \tag{29}$$

by introducing states $\mathbf{x}_{jk}$ governed by

$$\dot{\mathbf{x}}_{jk} = \mathbf{A}_{jk}\mathbf{x}_{jk} + \mathbf{B}_{jk}\dot{\eta}_k \tag{30}$$

The system matrices, $\mathbf{A}_{jk}, \mathbf{B}_{jk}, \mathbf{C}_{jk}, D_{jk}$, should be such that the frequency dependent added mass, $A_{jk}(\omega)$ and damping, $B_{jk}(\omega)$ can be replaced by the state space models. The procedure of obtaining these from the output files of VERES are automated by a MATLAB toolbox for frequency-domain identification, [12], and is used here. The vessel model then gets the form

$$\mathbf{M}_0 \begin{bmatrix} \ddot{\mathbf{r}} \\ \dot{\boldsymbol{\omega}} \end{bmatrix} + \mathbf{B}_0 \begin{bmatrix} \dot{\mathbf{r}} \\ \boldsymbol{\omega} \end{bmatrix} + \mathbf{C}\boldsymbol{\eta} + \boldsymbol{\mu} - \mathbf{b}_0 = \begin{bmatrix} \mathbf{f}^w \\ \mathbf{n}^w \end{bmatrix} \tag{31}$$

The fluid memory has a large impact on the vessel behaviour, as can be seen in figure 3, where the marine craft, i.e. body 0, is simulated with and without the fluid memory term. Hence, even though we require additional states (for our FDI process, we found seven 4th order models and six 3rd order models to represent the frequency variation in added mass and damping) which increases the simulation time significantly, we should always include it when analyzing vessel response in waves.

F. Wave Loads

The wave loads output files calculated by VERES are given in terms of force transfer functions, or *response amplitude operators* (RAOs). They are given as a ratio between forces and wave amplitudes, and cannot be used directly. In fact, considerable code is needed, so we rather rely on work done by others, and use the MSS toolbox [13], and in particular, the wave model and wave loads block written by Fossen and Smogeli. This toolbox is convenient for simulating marine crafts, and includes interface for working with data generated by VERES. In this toolbox, Fossen uses a differently defined body-frame than we do, so we restrict its use to generate wave loads. The wave models in MSS are stochastic and formulated as a wave spectrum $S(\omega, \psi)$, where ω is the wave frequency and ψ is the encounter angle of the waves relative to the ship. The well known frequency spectrum JONSWAP is used in this paper, with significant wave height of 2 m, and peak wave period 8 sec. The wave loads for all vessel coordinates are then interpolated to fit with the crane-vessel simulation.

G. System Equations

Now we have consistent acceleration terms for all our bodies, and can append the marine craft to the crane model.

$$\begin{bmatrix} \mathbf{M}_0 & & & \\ & \mathbf{M}_1 & & \\ & & \ddots & \\ & & & \mathbf{M}_9 \end{bmatrix} \begin{bmatrix} \dot{\mathbf{v}}_0 \\ \dot{\mathbf{v}}_1 \\ \vdots \\ \dot{\mathbf{v}}_9 \end{bmatrix} + \mathbf{b}(\mathbf{v}, \mathbf{q}) = \mathbf{g} \tag{32}$$

where the index denotes the body, $\mathbf{v}$ denotes all velocities and $\mathbf{q}$ denotes all coordinates, both stacked in tall column vectors. Also, $\mathbf{b}$ includes all terms that are not acceleration dependent and the right-hand side, $\mathbf{g}$ is a tall column vector of all external forces and moments and all reaction forces and moments. The form of the two are illustrated by

$$\mathbf{b} = \begin{bmatrix} \mathbf{B}_0\mathbf{v}_0 + \mathbf{C}\boldsymbol{\eta} + \boldsymbol{\mu} - \mathbf{b}_0 \\ \begin{bmatrix} \mathbf{0} \\ \tilde{\boldsymbol{\omega}}_1\mathbf{J}_1\boldsymbol{\omega}_1 \end{bmatrix} \\ \vdots \\ \begin{bmatrix} \mathbf{0} \\ \tilde{\boldsymbol{\omega}}_9\mathbf{J}_9\boldsymbol{\omega}_9 \end{bmatrix} \end{bmatrix}, \mathbf{g} = \begin{bmatrix} \begin{bmatrix} \mathbf{f}_0 \\ \mathbf{n}_0 \end{bmatrix} \\ \vdots \\ \begin{bmatrix} \mathbf{f}_9 \\ \mathbf{n}_9 \end{bmatrix} \end{bmatrix} \tag{33}$$

The appended system (32) is written in compact form as

$$\mathbf{M}\dot{\mathbf{v}} + \mathbf{b}(\mathbf{v}, \mathbf{q}) = \mathbf{g}^{\text{ext}} + \mathbf{g}^c \tag{34}$$

and, as we did for the single constrained body, in equations (6, 7, 9), we can express the constraint forces in terms of the constraint Jacobian and append kinematical relationships to obtain

$$\begin{bmatrix} \mathbf{M} & -\mathbf{D}^T \\ \mathbf{D} & \mathbf{0} \end{bmatrix} \begin{bmatrix} \dot{\mathbf{v}} \\ \boldsymbol{\lambda} \end{bmatrix} = \begin{bmatrix} \mathbf{g}^{\text{ext}} - \mathbf{b} \\ \boldsymbol{\gamma} \end{bmatrix} \tag{35}$$

III. Simulations

A. Numerical Simulations

The geometry and overall inertia properties of the crane is based on a 250 ton, active heave compensated knuckle boom crane. To obtain representative moments of inertia for the individual bodies, 3D models of each body were made and given accurate measurements according to 2D drawings, and given the same total mass. The moments of inertia were then calculated by our CAD software, based on a defined center of mass and on the assumption of homogeneous material density. The total weight of the crane is approximately 390 tons.

The ship geometry and displacement is also based on representative data and matches a real-case scenario

of a crane-carrying vessel. The vessel mass is about 14,000 tons, with a length, breadth and draught of 115, 25, and 6.4 meters, respectively. The hydrodynamic and hydrostatic parameters for the vessel are taken from pre-simulations using VERES. The fluid memory approximation and wave loads are all based on VERES calculations, but have been post-processed by the MSS toolbox to be directly applicable for a multibody simulation. The wave model is entirely due to MSS.

The payload is chosen as a $(6 \times 6 \times 4)$ meter box, with uniform density resulting in a mass of 10 tons. The attachment point of the payload is at the centroid of the top side, through a spherical joint. This leads to additional rotational motions of the payload, and hence makes the stabilization more challenging.

The cylinder control forces and the control torque for the revolute joint between the tower (body-1) and the king (body-2) are supplied by state feedback control. For the cylinders, the references are cylinder stroke and stroke velocity. For the revolute joint, the references are relative angle between bodies 1 and 2, and the relative rate of change of that angle.

To avoid excessive initial oscillations of the vessel due to the impact from gravitational forces from the crane and payload, we supply initial forces and moments to the vessel, thereby balancing the weight of the crane and the moment from that weight. Similarly, we supply initial forces to the cylinders and torque to the joint at point A, to avoid unnecessary computation time to stabilize the simulation from initial accelerations due to gravity. One of the advantages of the Newton-Euler method is that any force can easily be obtained by defining driver constraints which can be appended to the kinematic constraints to give a fully actuated model. This enables us to solve the kinetics using pure algebraic relations, and initial forces corresponding to any pose is easily found.

B. Results

The results section will include three cases to show the success of the simulation platform. In describing these, the parameters θ, s_1 and s_2 are the rotation angle of the crane base, and the strokes of the cylinders:

- Case 1: Crane without payload
  $\theta = -90°$, $s_1 = 2\text{m}$, $s_2 = 2\text{m}$
- Case 2: Crane with payload
  $\theta = -90°$, $s_1 = 2\text{m}$, $s_2 = 2\text{m}$
- Case 3: Crane without payload
  $\theta = -90°$, $s_1 = s_2 = 3 + \sin(2\pi/5t)$

The wave model used here is stochastic, but the same response and hence the same wave loads are used for all simulations. As a reference, these waveloads are applied to a single-body model of the marine craft. The figure 3 shows the vessel response in all coordinates - with and without the fluid memory model. Note that the inertial frame, $\{i\}$ is located at the point that initially is coincident with the point V. The body-fixed vessel frame, $\{0\}$, is initially located at $(33, 10, -10)$m.

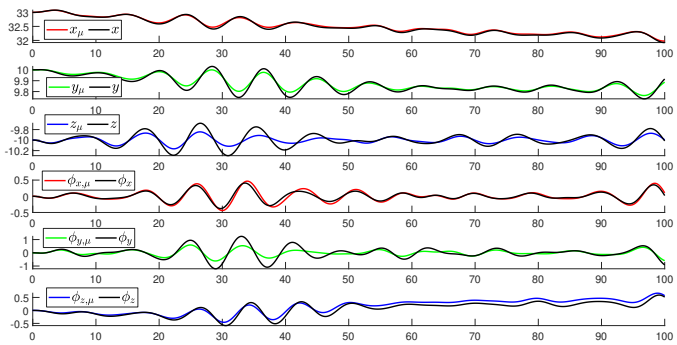

Figure 3: Vessel response - with and without $\boldsymbol{\mu}$
From top to bottom: Surge, sway, heave, roll, pitch, yaw. The units on the x-axis is seconds. The units on the y-axes are meters and degrees.

Figure 4 shows the initial and final configuration of the crane/vessel/payload for Case 2.

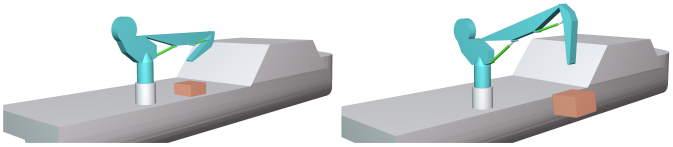

Figure 4: Figure showing initial and final pose of crane

The simulation is carried out for 100 sec, and the crane finishes its relative motion within 50 sec. The vessel is gently impacted by the payload in translational directions. Figure 5 shows the surge, sway and heave for cases 1 and 2.

By comparing the results with and without the crane, i.e. by looking at figure 6 vs figure 3, we see that the crane affects the vessel in the roll angle in particular. Also, the roll angle is significantly impacted by the payload, as expected. We also see that the yaw angle is affected by the reaction moment from the crane as the crane decelerates approaching the $-90°$ point around 40 seconds of simulation time.

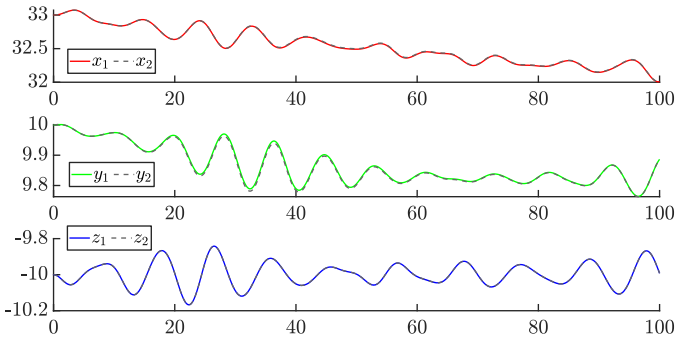

Figure 5: Surge, sway and heave for cases 1 and 2. Units are meters vs seconds.

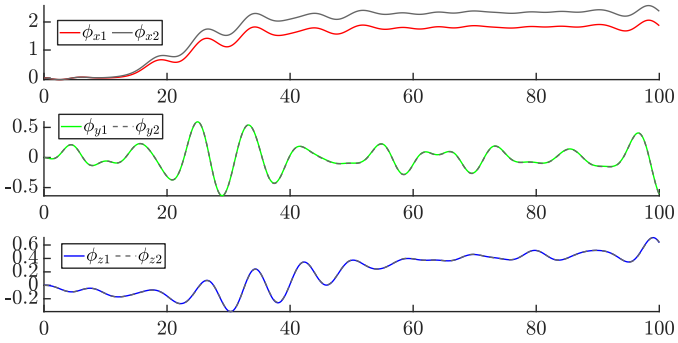

Figure 6: Roll, pitch and yaw for cases 1 and 2. Units are degrees vs seconds.

During the first 50 seconds of simulation time for the third case, we perform the same $0 \rightarrow -90°$ rotation of the base, and simultaneously extract both cylinders $0\text{m} \rightarrow 4\text{m}$. During the next 50 seconds, both cylinders start to follow a sinusoidal reference, $s = \cos(2\pi t/5)$ m, about the $s = 3$ m point. The sinusoidal motion references for the cylinders are included in order to generate distinctive crane kinetics that will be coupled to the vessel response, and hence be visually identifiable in the motion response of the vessel.

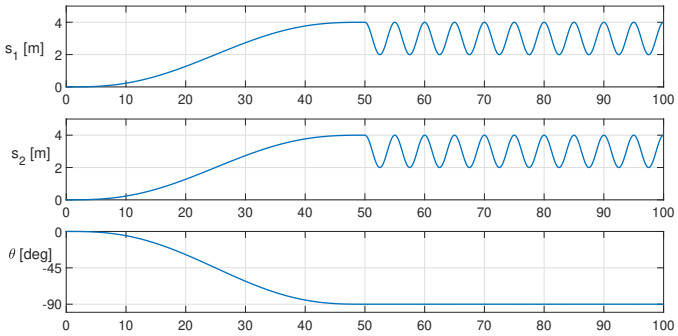

Figure 7: Cylinder strokes and crane orientation, case 3

The upper two rows of figure 7 show the norm of the vectors $\mathbf{r}_4 - \mathbf{r}_3$ and $\mathbf{r}_7 - \mathbf{r}_6$, i.e. the strokes of the cylinders, and the lower row shows the difference between the Euler angles about the local z-axes of bodies 1 and 2, $\phi_{z,2} - \phi_{z,1}$, during the simulation of case 3.

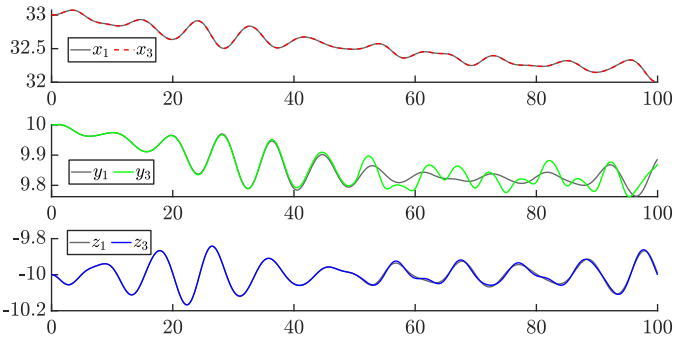

Figure 8: Surge, sway and heave for cases 1 and 3. Units are meters vs seconds.

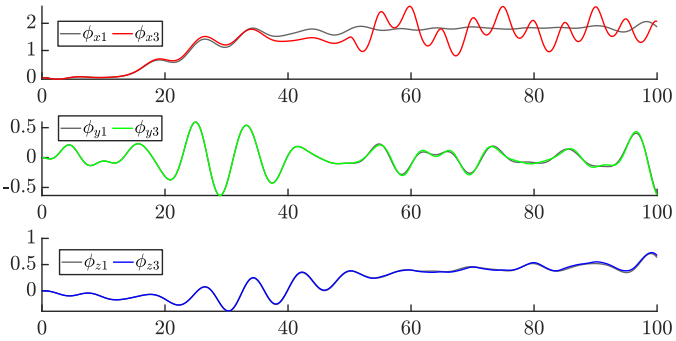

Figure 9: Roll, pitch and yaw for cases 1 and 3. Units are degrees vs seconds.

Figures 8 and 9 show the translational and rotational coordinates for the vessel during cases 1 and 3. By comparing these figures against the relative crane motions shown in figure 7, we can visually see how each individual degree of freedom of the vessel is impacted by the crane dynamics. For the translational coordinates, the sinusoidal crane kinetics is coupled the strongest with the sway direction. This is physically feasible since the crane is oriented towards the port side, and the reaction forces between the crane and vessel should have only minor components in the surge direction. Furthermore, although less visually obvious, the heave direction is also impacted by the sinusoidal crane kinetics. This can be seen more clearly in figure 10, where the difference in heave motions, $z_3 - z_1$ is plotted in meters. For the rotational coordinates, we expect a strong coupling of the sinusoidal crane kinetics in the roll direction - which is evident from the top row of figure 9.

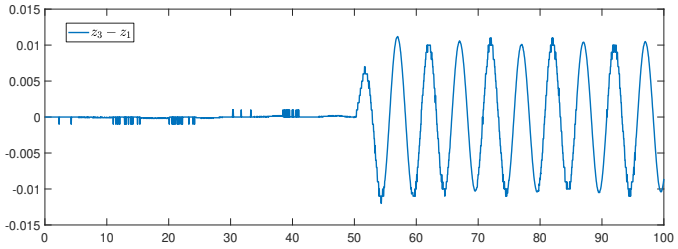

Figure 10: Difference in heave motion for cases 1 and 3. Units are meters vs seconds.

Finally, our simulation study has shown that even relatively small payloads, e.g. 10 metric tons compared to the max load 250 tons, will have an impact on the vessel stability when no further stabilization measures for the vessel are initiated.

IV. Conclusion

In this paper, we have derived and simulated a fully coupled rigid-body model of a knuckle-boom crane with payload and a marine craft. The final model consists of ten rigid bodies, including the payload. Hydrodynamic parameters and force RAOs based on the vessels geometry and inertia properties are included, and the applied wave loads are generated by a stochastic wave model using the JONSWAP wave spectrum. Frequency dependencies on hydrodynamic parameters of the vessel are accounted for by representing radiation forces by state space models, approximating the fluid memory term in the vessel equations of motion. The simulation results verify the effectiveness of the proposed methods.

The model can be used to determine reaction forces between individual members, e.g. to find the required cylinder forces to attain a certain trajectory, or to find the reaction forces between the crane and vessel operating in wave motion. Furthermore, it can readily be extended to include more dynamics, e.g. winch/wire and hydraulic actuation systems.

Acknowledgment

The research presented in this paper has received funding from the Norwegian Research Council, SFI Offshore Mechatronics, project number 237896.

References

[1] Y. Fang, P. Wang, N. Sun, and Y. Zhang, "Dynamic Analysis and Nonlinear Control of an Offshore Boom Crane," *IEEE Transactions on Industrial Electronics*, vol. 61, pp. 414–426, 2014.

[2] Y. Qian and Y. Fang, "Dynamic Analysis of an Offshore Ship-mounted Crane Subject to Sea Wave Disturbances," *IEEE World Congress on Intelligent Control and Automation*, pp. 1251–1256, 2016.

[3] B. Lu, Y. Fang, N. Sun, and X. Wang, "Antiswing Control of Offshore Boom Cranes with Ship Roll Distrurbances," *IEEE Transactions on Control Systems Technology*, vol. 26, pp. 740–747, 2018.

[4] K. Ellerman, E. Kreuzer, and M. Markiewitcz, "Nonlinear Dynamics of Floating Cranes," *Nonlinear Dynamics*, vol. 27, pp. 377–387, 2002.

[5] G. Tysse and O. Egeland, "Dynamic Interaction of a Heavy Crane and a Ship in Wave Motion," *Modeling, Identification and Control*, vol. 39, pp. 45–60, 2018.

[6] A. Cibicik, G. Tysse, and O. Egeland, "Determination of Reaction Forces of a Deck Crane in Wave Motion Using Screw Theory," *Journal of Offshore Mechanics and Arctic Engineering*, vol. 141, pp. 1–12, 2019.

[7] *VERES version 2.02.0837*, MARINTEK, Trondheim, Norway, 2017.

[8] N. Salvesen, E. Tuck, and O. Faltinsen, "Ship motions and sea loads," *The Society of Naval Architects and Marine Engineers*, 1970.

[9] P. E. Nikravesh, *Computer-Aided Analysis of Mechanical Systems*. Prentice Hall, 1988.

[10] E. J. Haug, *Computer-Aided Kinematics and Dynamics of Mechanical Systems*. Allyn and Bacon, 1989.

[11] E. Kristiansen, A. Hjulstad, and O. Egeland, "State-space representation of radiation forces in time-domain vessel models," *Ocean Engineering*, vol. 32, p. 2195–2216, 2005.

[12] T.Perez and T. Fossen, "A Matlab Toolbox for Parametric Identification of Radiation-Force Models of Ships and Offshore Structures," *Modelling, Identification and Control*, vol. 30, pp. 1–15, 2009.

[13] *Marine Systems Simulator*, T.I. Fossen and T. Perez, http://www.marinecontrol.org, 2017.